arXiv:2001.04999v1 [quant-ph] 14 Jan 2020

Non-Markovian super-superradiance in a linear chain of up to 100 qubits

Fatih Dinc[1,*] and Agata M. Brańczyk[1]

[1] *Perimeter Institute for Theoretical Physics, Waterloo, Ontario, N2L 2Y5, Canada*

We study non-Markovian enhancement effects in the spontaneous emission of a collective excitation in a linear chain of up to 100 qubits coupled to a 1D waveguide. We find that for a critical separation of qubits, the system exhibits super-superradiant (SSR) behavior leading to collective decay stronger than the usual Dicke superradiance. Here, time-delayed coherent quantum feedback effects are at play on top of the usual Dicke superradiance effects. We find a linear scaling for the SSR decay rate with increasing qubit number N such that $\Gamma_{\rm SSR} \sim 2.277 N\gamma_0$, where γ_0 is the single emitter decay rate to a one-dimensional waveguide, as opposed to $\Gamma_{\rm Dicke} \sim N\gamma_0$ for Dicke superradiance. The SSR decay rate can be tuned with qubit separation distance and may therefore have application for quantum technologies.

Surprising phenomena can emerge when multiple quantum systems coordinate their behaviour. A well-known example of this—Dicke superradiance [1, 2]—occurs when a group of N quantum emitters, excited in a symmetric state, exhibits *enhanced* spontaneous emission [3–5]. This phenomenon, predicted when the distance between emitters is small compared to the wavelength of radiation, can be understood as *collective* behaviour of the entire system. Curiously, enhanced emission can also occur when the emitters are macroscopically separated [6–9]; a regime in which collective behaviour might not be expected. What's more, the emission can become more enhanced than Dicke superradiance; earning it the name *super-superradiance* (SSR) [8]. This highly counter-intuitive phenomenon can be explained by an effect that has recently gained attention in other contexts [10–16]: *time-delayed coherent quantum feedback*. In this paper, we study the effects of time-delayed coherent quantum feedback on the *super-superradiant* collective decay rate of a linear chain of qubits coupled to a one-dimensional (1D) waveguide.

The 1D geometry of the waveguide enhances scattering and is thus particularly favourable to study time-delayed coherent quantum feedback. While linear chains of qubits in 1D waveguides have been studied extensively, both theoretically [9, 17–21] and experimentally [22–24], the literature mostly focuses on regimes where the Markovian approximation is valid, i.e. time retardation effects are negligible. Time-delayed coherent quantum feedback, however, occurs when qubits are separated by distances in which the Markovian limit is no longer valid. One must, therefore, take into account non-Markovian dynamics of qubit-light interactions. This was done in waveguide QED for a single qubit in [13, 25–27] for two qubits in [6, 7] and three qubits in [8]. Here, we consider up to 100 qubits.

We consider a linear chain of N identical qubits separated by a distance L and coupled to a 1D waveguide as shown in Fig. 1. We study SSR by computing the collective decay rates of the N-qubit system. Our method of choice is the real-space approach [8]. In this approach, one first identifies the transfer matrix for the system, then uses that matrix to write down and solve a characteristic equation for the collective decay rates. The real-space approach has the following strengths for this problem: (1) No need to model time-dynamics, as the collective decay rates can be found from steady-state single-frequency solutions (energy eigenstates for the whole system); (2) No need to identify the multi-qubit superposition states that corresponds to SSR (in fact, one does not need to consider the qubit excitation subspace at all); and (3) Energy eigenstates can be found via a recursive transfer matrix method. These strengths of the real-space approach make the problem significantly more tractable for large-N systems.

We start by identifying the transfer matrix. For a plane wave with frequency k, incident from far left, the transformation that relates the transmitted and reflected photon coefficients, t and r respectively, to the incident photon is

$$\begin{pmatrix} 1 \\ r \end{pmatrix} = T^N \begin{pmatrix} t \\ 0 \end{pmatrix}. \tag{1}$$

Here, T is the transfer matrix corresponding to a unit cell, which consists of inter-qubit propagation and single qubit-light interaction. Following [8], T can be written as

$$T = \begin{pmatrix} 1 + i\frac{\gamma_0}{2\Delta_k} & i\frac{\gamma_0}{2\Delta_k} \\ -i\frac{\gamma_0}{2\Delta_k} & 1 - i\frac{\gamma_0}{2\Delta_k} \end{pmatrix} \begin{pmatrix} e^{-ikL} & 0 \\ 0 & e^{ikL} \end{pmatrix}, \tag{2}$$

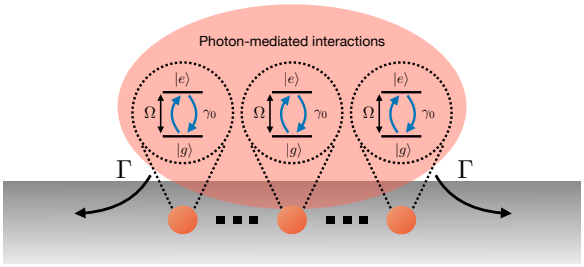


FIG. 1. The linear chain of N qubits coupled to a 1D waveguide. The photon-mediated interactions between qubits lead to a collective behavior of the system described by collective decay rates. An initially excited system decays through these decay modes.

where L is the distance between two adjacent qubits, $\Delta_k = E_k - \Omega$ is the detuning between the photon energy E_k and the qubit energy separation Ω, and γ_0 is the decay rate of a single qubit to the 1D waveguide. When deriving this transfer matrix, we use the real-space Hamiltonian [8, 20, 28], where the light-matter interactions take the form of a delta-function at the qubit position. For the scope of this paper, we assume $\gamma_0/\Omega \ll 1$ in alignment with the rotating-wave approximation performed at the Hamiltonian level. For the remainder of this paper, we set $\hbar = 1$ and $v_g = 1$, where v_g is the group velocity of the photons inside the waveguide.

We now determine the characteristic equation for the collective decay rates by setting the first element of the transfer matrix in (1) to zero: $(T^N)_{11} = 0$. The decay rates, Γ, can then be obtained via a complex rotation followed by a scaling from the poles $\Delta_k^{(p)}$ of the scattering parameters, i.e., $\Gamma = 2i\Delta_k^{(p)}$ [8] (the real part of Γ corresponds to the physical decay rate and the imaginary part is responsible for a characteristic frequency shift). The factor of 2 comes from the fact that we are interested in population decay rates. With this definition, the characteristic equation of the poles for an N qubit system is

$$f(\Delta_k) = \Delta_k^N (T^N)_{11}, \tag{3}$$

where the multiplication with Δ_k^N results in a characteristic equation that is polynomial in Δ_k and e^{ikL} (hence analytic in the complex plane). As a result, the problem of finding the collective decay rates comes down to finding the roots of the function $f(\Delta_k)$. Solving this characteristic equation for a single qubit and performing the rotation, we find the single emitter decay rate to be γ_0 as expected.

One can consider this problem of finding the collective decay rates in two different regimes: the Markovian regime in which the qubits are microscopically separated ($L \sim O(\Omega^{-1})$) and the propagation time of the photons within the system is negligible; and the non-Markovian regime in which the qubits are macroscopically separated ($L \sim O(\gamma_0^{-1})$) and the propagation time of the photons within the system is not negligible. The superradiance condition in both regimes is $\Omega L = \pi n$, where n is an integer [8, 9].

In the Markovian regime, the propagation phase acquired by the photon between two qubits can be linearized, $kL \simeq \Omega L$ [6, 8]. In this regime, $f(\Delta_k)$ can be approximated by an Nth degree polynomial in Δ_k, since the exponential terms in the transfer matrix can be replaced by a constant $e^{ikL} \simeq e^{i\Omega L}$. The N zeros, which correspond to N collective decay rates, can be found analytically. When the superradiant condition is satisfied, the superradiant decay rate is $N\gamma_0$ and all other decay rates are zero [8]. This is the case of Dicke superradiance.

In the non-Markovian regime, the photon's propagation phase can no longer be linearized, so the Markovian approximation is no longer valid. In this regime, $f(\Delta_k)$ can no longer be approximated by a polynomial (it depends on $e^{ikL} = e^{i\Omega L(1+\Delta_k/\Omega)}$ as well). Relaxing the linearization condition leads to time-retardation effects inside the multi-qubit system. A discussion on how the linearization $kL \simeq \Omega L$ is linked to the Markovianity assumption can be found in [8] (in particular, in Sections VI and VIII). Consequently, $f(\Delta_k)$ has infinitely many zeros that correspond to infinitely many collective decay rates, which can be divided into two categories: those that tend to Markovian decay rates in the limit $L \to 0$ (we call these Markovian-like) and those that tend to infinity in the same limit (we call these exclusively non-Markovian).

SSR refers to the phenomenon that a Markovian-like decay rate surpasses the Dicke superradiance decay rate $\Gamma_{\text{Dicke}} = N\gamma_0$. To achieve maximum SSR, the qubits must be separated by a critical distance L_c (as pointed out in [7]) as well as satisfy the condition $\Omega L_c = n\pi$. For any L and $\Omega L = n\pi$, $f(\Delta_k)$ has $N-1$ zeros that correspond to $\Gamma = 0$ (this occurs when $\Delta_k = 0$). This leaves only one Markovian-like decay rate which could potentially become SSR, i.e. the non-zero Γ closest to the origin.

In our analysis, we therefore first assume that $\Omega L = n\pi$ and set $e^{ikL} = e^{i\Omega L(1+\Delta_k/\Omega)} = (-1)^n e^{i\Delta_k L}$. We then use a numerical root finding

algorithm to find the first N zeros of $f(\Delta_k)$ that are closest to the origin. $N-1$ of such zeros are found to be within the vicinity of $\Delta_k = 0$, deviating only by small amounts due to numerical imprecision. The Nth zero, labelled as p, gives the superradiant decay rate via the Wick-like rotation $\Gamma_u = 2ip$. The real part of Γ_u gives the physical decay rate. We define the SSR decay rate as $\Gamma_{\rm SSR} = \max_L \mathrm{Re}[\Gamma_u]$, and perform the maximization numerically. As a sanity check, we then plot $\log(|f(\Delta_k)|)$ for Δ_k near $\Gamma_{\rm SSR}$ and compare it with the values found numerically.

Fig. 2 shows the symmetric and anti-symmetric decay rates (i.e. those that couple to symmetric and anti-symmetric superposition states) for $N = 2$ qubits in the non-Markovian regime as a function of qubit separation L for finite Ω, enveloped by an upper bound given by $\Omega \to \infty$ (for $L = 0$, the symmetric decay rate couples to the Dicke state). The symmetric and anti-symmetric decay rates follow the same trend as in Fig. 4(d) of [6]. The numerical values $\Gamma_{\rm SSR} \approx 4.59\gamma_0$ and $L_c \approx 0.56\gamma_0^{-1}$ match perfectly with the findings of [7]. When the condition $\Omega L_c = n\pi$ is satisfied, the peak of the curve for the symmetric decay rate lines up with the peak of the dashed blue envelope function, as is the case in Fig. 2. If the condition is not satisfied, the system acquires a maximum decay for a distance closest to L_c.

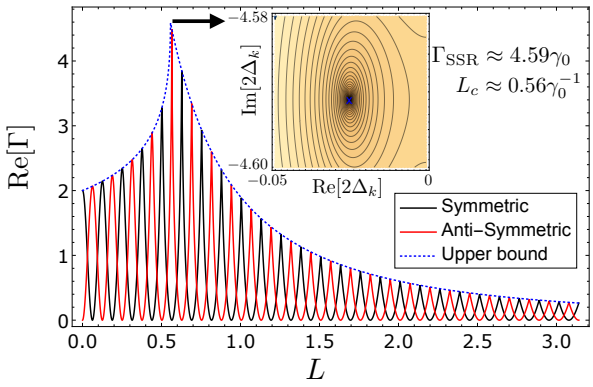


FIG. 2. The physical decay rate, given by the real part of Γ (in units of γ_0) for $N = 2$ qubits in the non-Markovian regime as a function of qubit separation L (in units of γ_0^{-1}). Black ($\mathrm{Re}[\Gamma] = 2\gamma_0$ at $L = 0$) and red lines ($\mathrm{Re}[\Gamma] = 0$ at $L = 0$) correspond to symmetric and anti-symmetric decay rates for $\Omega = 50\gamma_0$. The dashed blue line gives the upper bound obtained in the limit $\Omega \to \infty$ of the superradiant decay values. All numerical values are normalized w.r.t. γ_0. Inset: $\log(|f(\Delta_k)|)$ for $L = L_c$ for Δ_k close to the SSR pole.

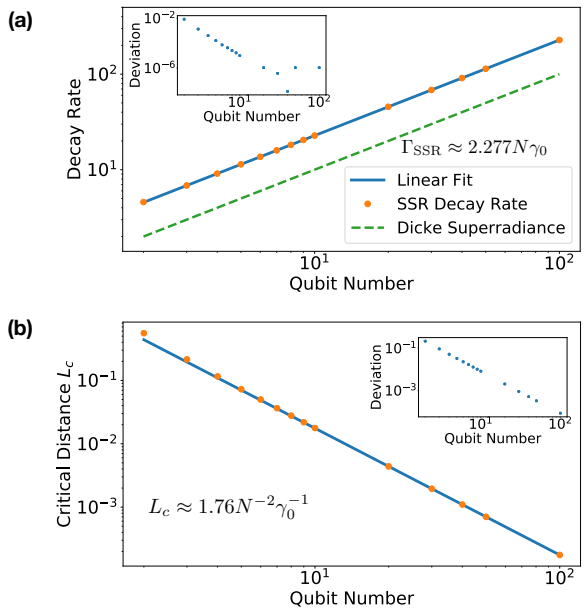


FIG. 3. The scaling of (a) the SSR decay rate $\Gamma_{\rm SSR}$ and (b) the critical distance L_c w.r.t. the qubit number N. The inset figures show the relative deviation between the fit and the numerical values ($\left|\frac{\text{fit}-\text{data}}{\text{data}}\right|$). The uncertainty in the scaling of the SSR decay rate is well within the errors of the numerical maximization algorithm, whereas for the critical distance there is a significant deviation from the fit even in large N. We note that, unlike Dicke superradiance, the SSR does not scale exactly linearly for small N. There is a significant difference for $N \leq 10$ between the fit and the numerical data.

We now ask whether SSR is a general phenomenon that persists beyond the known cases of $N = 2$ and $N = 3$. To answer this, we repeat the above analysis for various N up to $N = 100$. We find that indeed SSR persists for large N and that $\Gamma_{\rm SSR}$ scales linearly, as shown in Fig. 3 (a). The scaling is similar to that of Dicke superradiance. Fig. 3 (b) shows how the critical distance L_c scales with N. The fit is almost linear, but deviates for $N < 10$.

To study the closeness of the linear fits, we plot the deviation of the numerical results in Fig. 3. For $\Gamma_{\rm SSR}$, the deviation hovers around $\sim 10^{-6}$ for large N, which is within the numerical precision of our algorithm. For L_c, the fit is not as close: the N^{-2} scaling fits the data within 0.1%. For more evidence for this scaling, we turn to analytical investigations.

A closed form solution exists for the transmission and reflection coefficients related by the transfer matrix as in (1) [20]. Applying the superradiant con-

dition $\Omega L = \pi n$, the characteristic set of equations corresponding to the poles becomes

$$\cos(\lambda) = \cos(pL) + \frac{\gamma_0}{2p}\sin(pL), \quad \text{(4a)}$$

$$(p + i\gamma_0/2)\sin(\lambda N) = e^{ipL}p\sin(\lambda(N-1)). \quad \text{(4b)}$$

Here, λ is a complex number that relates both equations and p relates to the collective decay rate as $\Gamma = 2ip$. Now, let us set $p = -i\frac{\alpha}{2}N\gamma_0$ ($\Gamma = \alpha N\gamma_0$) and $L = \beta N^{-2}\gamma_0^{-1}$ from the numerical fit we obtained in Fig. 3. Here, the pair (α, β) are free parameters to be determined. Then, neglecting terms of order $O(N^{-1})$, the set of equations in (4) becomes

$$g(\alpha, \beta) = 2\alpha\tau\cosh(\tau) - (2 + \alpha^2\beta)\sinh(\tau) = 0, \quad (5)$$

with $\tau = 0.5\sqrt{\beta(4 + \alpha^2\beta)}$. We note that the coefficient of $O(N^{-1})$ term is nonzero, which explains the deviations for $N < 10$. The SSR decay rate scales asymptotically for large N in contrast to the exact scaling of the Dicke-superradiance. There are infinitely many (α, β) pairs that satisfy this equation, which has been illustrated in Fig. 4. The most important observation is that there exists a β_c such that there is no solution [29] to $g(\alpha, \beta) = 0$ for $\beta > \beta_c$ and there are two pairs $(\alpha_{s/l}, \beta)$ (s/l stand for small/large) for $\beta < \beta_c$. In this case, the Markovian-like decay rate scales as $\Gamma_u = \alpha_s N\gamma_0$ and the $N+1$th (exclusively non-Markovian) decay rate scales as $\Gamma_{\rm NM} = \alpha_l N\gamma_0$. As $\beta \to \beta_c$, both Γ_u and $\Gamma_{\rm NM}$ come closer and right at $\beta = \beta_c$, Γ_u is maximized and has the same real part as $\Gamma_{\rm NM}$. Consequently, $\Gamma_{\rm SSR} = \max_L \mathrm{Re}[\Gamma_u]$ is obtained at the position $\frac{\partial g(\alpha,\beta)}{\partial \alpha} = 0$. This corresponds to the condition $\alpha_c\beta_c = 4$, with c standing for the critical values. The characteristic equation can be solved for this condition and the resulting $(\alpha_c, \beta_c) \approx (2.277, 1.76)$ pair agrees with the numerical fit in Fig. 3, confirming our numerical analysis. It is important to note that the crucial step here is the Ansatz that $p \sim N\gamma_0$ and $L \sim N^{-2}\gamma_0^{-1}$, which was obtained from the numerical analysis in the first place.

This analytical investigation also explains another interesting phenomenon. The imaginary part of $\Gamma_{\rm SSR}$ is responsible for the collective energy level shifts. For $L \ll L_c$, the superradiant decay rate Γ_u is strictly real and does not have an imaginary component, whereas the $N+1$th exclusively NM collective decay rate is negligibly far away from the origin. This justifies the N-pole approximation performed in [6], where the $N+1$th pole is so far away from the first N such that it can be neglected. However, for $L > L_c$, the Nth and $N+1$th decay rates become degenerate. They have the same real parts, but also imaginary parts with the opposite sign. The fact that the decay rates acquire imaginary components for $L > L_c$ suggests a shift in collective energy levels analogous to the Lamb shift. A similar observation has been made in [6] for $N = 2$ qubits. Furthermore, we point to another interesting phenomenon. The energy levels corresponding to the Nth closest pole to the origin changes discontinuously around the superradiant condition $\Omega L = n\pi$ with changing L for $L > L_c$. This has been plotted in Fig. 4 of [6] for $N = 2$, where increasing the distance between qubits can lead to discontinues changes in the energy level shifts around L values where $\Omega L = n\pi$. We observe here that this is a more general phenomenon for any N. We plan to investigate the shifts in the collective energy levels due to non-Markovian effects further in future work.

In summary, the SSR decay rate scales linearly ($\Gamma_{\rm SSR} \sim N\gamma_0$) and the critical qubit separation scales by the inverse square ($L_c \sim N^{-2}\gamma_0^{-1}$). While the time-delayed quantum coherent feedback leads to a stronger decay of the collective system, the scaling of the decay rate is still linear with increasing N. Furthermore, while $\Gamma_{\rm Dicke} \sim N\gamma_0$ fits exactly for any N in the case of the Dicke superradiance, the value $\Gamma_{\rm SSR} \sim 2.277N\gamma_0$ fits well asymptotically for large N. We don't yet know the origin of the linear scaling but we hope to investigate this interesting phenomenon further. As a starting point, it is important to realize that the overall size of the system is $\approx NL_c \sim 1.76N^{-1}\gamma_0^{-1} \ll \gamma_0^{-1}$. This means that light initially emitted by a qubit at one end of the chain travels all the way to the other end and back in less time than the half-time of that individual qubit. Consequently, even photon-mediated interactions between the first and Nth qubits are in fact significant in the emergence of the SSR phenomenon. Conversely, when qubits are separated by large distances, the collective decay rates become subradiant in agreement with the findings of [6]. Hence, SSR is only observed when the qubits are moderately separated ($L \approx L_c$), where both collective interactions and time-retardation effects are at play.

When it comes to applications, the non-Markovian system provides additional control parameters. In Markovian 1D waveguide QED, the decay rates depend on the coupling and the phase

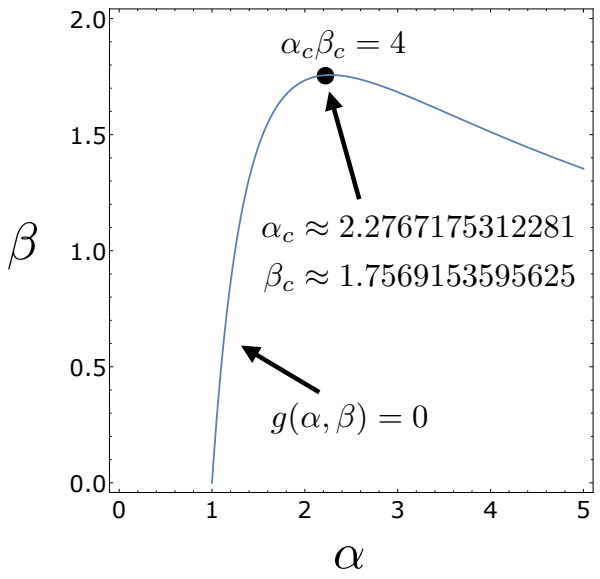


FIG. 4. The contour plot of $g(\alpha, \beta) = 0$. Here, the assumption $\Delta_k = -i0.5\alpha N\gamma_0$ and $L_c = \beta N^{-2}\gamma_0^{-1}$ is valid as long as we pick a pair (α, β) on the contour. For $\beta > \beta_c$, there is no such pair. For $\beta < \beta_c$, there are two such pairs corresponding to two distinct poles (one exclusively non-Markovian, one Markovian-like). The pole with smaller α corresponds to Γ_u, but is not the SSR decay rate since larger α can be achieved for $\Gamma_u = \alpha N\gamma_0$ (and $\Gamma_{\rm SSR} = \max_\beta \mathrm{Re}[\Gamma_u]$). For $\beta = \beta_c$, there is only one such pair, corresponding to $\Gamma_{\rm SSR}$ and L_c. Note that for the pair (β_c, α_c), the equation $\alpha_c\beta_c = 4$ is an exact one.

parameter ΩL. In the non-Markovian regime, however, the decay rates also depend on the qubit separation L and frequency Ω independently. Furthermore, the distance can enhance the decay rate beyond Dicke superradiance. By tuning the qubit separation, one can tune the interaction between photons and multi-qubit systems, which might have application for quantum technologies such as quantum memories [30–32], quantum gates [33] and pulse shaping [8]. Furthermore, our formalism makes it possible to study systems with many qubits. We thus expect our approach to be useful for designing new quantum technologies.

Research at the Perimeter Institute is supported by the Government of Canada through the Department of Innovation, Science and Economic Development Canada, and by the Province of Ontario through the Ministry of Research and Innovation. We acknowledge the support of the Natural Sciences and Engineering Research Council of Canada (funding reference number RGPIN-2016-04135).

* Present adress: Department of Applied Physics, Stanford University, Stanford, CA, USA
Email: fdinc@stanford.edu

[1] Anatolii V Andreev, Vladimir I Emelyanov, and Yu A Ilinskiĭ. Collective spontaneous emission (dicke superradiance). *Soviet Physics Uspekhi*, 23(8):493–514, aug 1980.
[2] Robert H Dicke. Coherence in spontaneous radiation processes. *Physical review*, 93(1):99, 1954.
[3] Romain Fleury and Andrea Alu. Enhanced superradiance in epsilon-near-zero plasmonic channels. *Physical Review B*, 87(20):201101, 2013.
[4] Sajeev John and Tran Quang. Localization of superradiance near a photonic band gap. *Physical review letters*, 74(17):3419, 1995.
[5] Nipun Vats and Sajeev John. Non-markovian quantum fluctuations and superradiance near a photonic band edge. *Physical Review A*, 58(5):4168, 1998.
[6] Huaixiu Zheng and Harold U Baranger. Persistent quantum beats and long-distance entanglement from waveguide-mediated interactions. *Physical review letters*, 110(11):113601, 2013.
[7] Kanupriya Sinha, Pierre Meystre, Elizabeth A Goldschmidt, Fredrik K Fatemi, Steven L Rolston, and Pablo Solano. Non-markovian collective emission from macroscopically separated emitters. *arXiv preprint arXiv:1907.12017*, 2019.
[8] Fatih Dinc, İlke Ercan, and Agata M. Brańczyk. Exact Markovian and non-Markovian time dynamics in waveguide QED: collective interactions, bound states in continuum, superradiance and subradiance. *Quantum*, 3:213, December 2019.
[9] Yao Zhou, Zihao Chen, and Jung-Tsung Shen. Single-photon superradiant emission rate scaling for atoms trapped in a photonic waveguide. *Physical Review A*, 95(4):043832, 2017.
[10] Arne L Grimsmo. Time-delayed quantum feedback control. *Physical review letters*, 115(6):060402, 2015.
[11] Pierre-Olivier Guimond, Mikhail Pletyukhov, Hannes Pichler, and Peter Zoller. Delayed coherent quantum feedback from a scattering theory and a matrix product state perspective. *Quantum Science and Technology*, 2(4):044012, 2017.
[12] Hannes Pichler and Peter Zoller. Photonic circuits with time delays and quantum feedback. *Physical review letters*, 116(9):093601, 2016.
[13] Giuseppe Calajó, Yao-Lung L Fang, Harold U Baranger, Francesco Ciccarello, et al. Exciting a bound state in the continuum through multiphoton scattering plus delayed quantum feedback. *Physical Review Letters*, 122(7):073601, 2019.
[14] Hannes Pichler, Soonwon Choi, Peter Zoller, and Mikhail D Lukin. Universal photonic quantum com-

putation via time-delayed feedback. *Proceedings of the National Academy of Sciences*, 114(43):11362–11367, 2017.

[15] SJ Whalen, AL Grimsmo, and HJ Carmichael. Open quantum systems with delayed coherent feedback. *Quantum Science and Technology*, 2(4):044008, 2017.

[16] Hamidreza Chalabi and Edo Waks. Interaction of photons with a coupled atom-cavity system through a bidirectional time-delayed feedback. *Physical Review A*, 98(6):063832, 2018.

[17] Guo-Zhu Song, Ewan Munro, Wei Nie, Leong-Chuan Kwek, Fu-Guo Deng, and Gui-Lu Long. Photon transport mediated by an atomic chain trapped along a photonic crystal waveguide. *Physical Review A*, 98(2):023814, 2018.

[18] Sumanta Das, Vincent E Elfving, Florentin Reiter, and Anders S Sørensen. Photon scattering from a system of multilevel quantum emitters. ii. application to emitters coupled to a one-dimensional waveguide. *Physical Review A*, 97(4):043838, 2018.

[19] Zeyang Liao, Xiaodong Zeng, Shi-Yao Zhu, and M Suhail Zubairy. Single-photon transport through an atomic chain coupled to a one-dimensional nanophotonic waveguide. *Physical Review A*, 92(2):023806, 2015.

[20] T. S. Tsoi and C. K. Law. Quantum interference effects of a single photon interacting with an atomic chain inside a one-dimensional waveguide. *Physical Review A*, 78:063832, Dec 2008.

[21] Andreas Albrecht, Loïc Henriet, Ana Asenjo-Garcia, Paul B Dieterle, Oskar Painter, and Darrick E Chang. Subradiant states of quantum bits coupled to a one-dimensional waveguide. *New Journal of Physics*, 21(2):025003, 2019.

[22] A Goban, C-L Hung, JD Hood, S-P Yu, JA Muniz, O Painter, and HJ Kimble. Superradiance for atoms trapped along a photonic crystal waveguide. *Physical Review Letters*, 115(6):063601, 2015.

[23] Jonathan D Hood, Akihisa Goban, Ana Asenjo-Garcia, Mingwu Lu, Su-Peng Yu, Darrick E Chang, and HJ Kimble. Atom–atom interactions around the band edge of a photonic crystal waveguide. *Proceedings of the National Academy of Sciences*, 113(38):10507–10512, 2016.

[24] A Goban, C-L Hung, S-P Yu, JD Hood, JA Muniz, JH Lee, MJ Martin, AC McClung, KS Choi, Darrick E Chang, et al. Atom–light interactions in photonic crystals. *Nature communications*, 5:3808, 2014.

[25] Tommaso Tufarelli, M. S. Kim, and Francesco Ciccarello. Non-markovianity of a quantum emitter in front of a mirror. *Phys. Rev. A*, 90:012113, Jul 2014.

[26] Tomás Ramos, Benoît Vermersch, Philipp Hauke, Hannes Pichler, and Peter Zoller. Non-markovian dynamics in chiral quantum networks with spins and photons. *Physical Review A*, 93(6):062104, 2016.

[27] Yao-Lung L Fang, Francesco Ciccarello, and Harold U Baranger. Non-markovian dynamics of a qubit due to single-photon scattering in a waveguide. *New Journal of Physics*, 20(4):043035, 2018.

[28] Jung-Tsung Shen and Shanhui Fan. Coherent single photon transport in a one-dimensional waveguide coupled with superconducting quantum bits. *Physical Review Letters*, 95(21):213001, 2005.

[29] This has been checked for a large interval of α and β values numerically.

[30] H Jeff Kimble. The quantum internet. *Nature*, 453(7198):1023, 2008.

[31] Alexander I Lvovsky, Barry C Sanders, and Wolfgang Tittel. Optical quantum memory. *Nature photonics*, 3(12):706, 2009.

[32] Erhan Saglamyurek, Taras Hrushevskyi, Anindya Rastogi, Khabat Heshami, and Lindsay J LeBlanc. Coherent storage and manipulation of broadband photons via dynamically controlled autler–townes splitting. *Nature Photonics*, 12(12):774, 2018.

[33] Joshua Combes and Daniel J Brod. Two-photon self-kerr nonlinearities for quantum computing and quantum optics. *Physical Review A*, 98(6):062313, 2018.